HHS Public Access

Author manuscript

*Life Sci Space Res (Amst)*. Author manuscript; available in PMC 2023 March 07.

Published in final edited form as:

*Life Sci Space Res (Amst)*. 2023 February ; 36: 18–26. doi:10.1016/j.lssr.2022.11.001.

# Glycogen metabolism is required for optimal cyanobacterial growth in the rapid light-dark cycle of low-Earth orbit

**Bryan Bishé**,

**Susan S. Golden**,

**James W. Golden***

Department of Molecular Biology, University of California San Diego, 92093 La Jolla, CA, United States

## Abstract

Some designs for bioregenerative life support systems to enable human space missions incorporate cyanobacteria for removal of carbon dioxide, generation of oxygen, and treatment of wastewater, as well as providing a source of nutrition. In this study, we examined the effects of the short light-dark (LD) cycle of low-Earth orbit on algal and cyanobacterial growth, approximating conditions on the International Space Station, which orbits Earth roughly every 90 min. We found that growth of green algae was similar in both normal 12 h light:12 h dark (12 h:12 h LD) and 45′:45′ LD cycles. Three diverse strains of cyanobacteria were not only capable of growth in short 45′:45′ LD cycles, but actually grew better than in 12 h:12 h LD cycles. We showed that 45′:45′ LD cycles do not affect the endogenous 24 h circadian rhythms of *Synechococcus elongatus.* Using a dense library of randomly barcoded transposon mutants, we identified genes whose loss is detrimental for the growth of *S. elongatus* under 45′:45′ LD cycles. These include several genes involved in glycogen metabolism and the oxidative pentose phosphate pathway. Notably, 45′:45′ LD cycles did not affect the fitness of strains that carry mutations in the biological circadian oscillator or the clock input and output regulatory pathways. Overall, this study shows that cultures of cyanobacteria could be grown under natural sunlight of low-Earth orbit and highlights the utility of a functional genomic study in a model organism to better understand key biological processes in conditions that are relevant to space travel.

### Keywords

Cyanobacteria; Low-Earth orbit; Bioregenerative life support; Circadian rhythms



*Corresponding author. jwgolden@ucsd.edu (J.W. Golden).

Declaration of Competing Interest

The authors declare that they have no known competing financial interests or personal relationships that could have appeared to influence the work reported in this paper.

Supplementary materials

Supplementary material associated with this article can be found, in the online version, at doi:10.1016/j.lssr.2022.11.001.

## 1. Introduction

One of the challenges and opportunities for spaceflight research is developing in-situ resource utilization to support a human presence in space. This ability will be increasingly important as crewed missions become longer and venture farther from Earth. Since 2001 the International Space Station (ISS) has hosted a continuous human presence in low-Earth orbit (LEO) with life support functions provided by physical-chemical (P-C) systems (Keller et al., 2021). Humans on the ISS rely on constant resupply missions for food and non-renewable P-C resources that will be much more difficult and costly for longer duration missions with destinations such as the Moon or Mars. Bioregenerative life support systems (BLSS) will need to be developed and replicate various functions of the P-C systems that remove carbon dioxide, generate oxygen, and recycle water. In addition, BLSS may be further utilized to generate food and fuel required for those longer missions.

Cyanobacteria comprise a large family of photoautotrophic bacteria and are well qualified to perform key functions to support human space exploration. Fossils composed of cyanobacteria are some of the oldest known records of life on Earth, and cyanobacteria are the only organisms to have evolved oxygenic photosynthesis (Martin and Kowallik, 1999; Schirrmeister et al., 2015). Cyanobacteria are ubiquitous in all sunlit environments on Earth and gave rise to chloroplasts, which are photosynthetic organelles present in cells of higher plants and algae (Schirrmeister et al., 2015; Shih et al., 2013). Cyanobacteria are resistant to both desiccation and UV exposure and can even survive exposure to space conditions in LEO (Song et al., 2016; De et al., 2019; Cottin and Rettberg, 2019).

Through oxygenic photosynthesis, cyanobacteria both remove $CO_2$ from the air and generate oxygen, reactions that are handled by separate P-C systems on current spaceflight missions (Keller et al., 2021). The fixed $CO_2$ is used to produce all of the organic molecules required for growth and the oxygen is released as a byproduct of photosynthesis. The European Space Agency's closed-loop Micro-Ecological Life Support System Alternative (MELiSSA) relies on cyanobacteria not only for $CO_2$ removal and oxygen generation, but also to process wastewater to remove nitrogen and phosphorous compounds and generate edible biomass (Hendrickx et al., 2006). A recent experiment successfully cultured cyanobacteria in a bioreactor on the ISS and showed that biomass production was similar in microgravity and ground conditions (Poughon et al., 2020).

To save energy, cyanobacteria in space could be cultured using ambient sunlight. However, most eukaryotic organisms as well as cyanobacteria have an internal biological clock that keeps approximately 24 h circadian time (Cohen and Golden, 2015), and the light-dark (LD) cycles of LEO are very different than the 24 h LD cycles at the Earth's surface. The ISS orbits roughly once every 90 min, rapidly moving in and out of sunlight 16 times over 24 h. This period of lighting is highly unusual for organisms that evolved in a consistent 24 h day-night cycle and maintain an internal molecular clock with a roughly 24 h period that regulates cellular metabolism and activity. Circadian clocks are ancient mechanisms that synchronize cellular activities with the Earth's day-night cycle in eukaryotic organisms including plants and humans (Inoue et al., 2018; Ode and Ueda, 2018). Prokaryotes were once thought to be too simple to encode such a complicated

mechanism, but circadian clocks were discovered more than 35 years ago in cyanobacteria (Cohen and Golden, 2015). The most extensively studied bacterial circadian clock is in the cyanobacterium *Synechococcus elongatus* PCC 7942 (hereafter *S. elongatus*) (Golden, 2020). The *S. elongatus* core circadian oscillator is composed of three proteins, KaiA, KaiB, and KaiC, with other regulatory elements acting as inputs that set the clock and outputs that control cellular activities by regulating gene expression (Ishiura et al., 1998; Schmitz et al., 2000).

In this study, we investigated the effects of the rapid day-night transitions of LEO on the survival and growth of green algae and cyanobacteria. Using the genetic tools available for a model cyanobacterial strain, we examined the effects of this 45 min light:45 min dark (45′:45′ LD) exposure on the cell's internal circadian rhythms and identified genes whose loss of function affect the oxidative pentose phosphate pathway and negatively impact cell growth. Overall, we found that cyanobacteria are able to thrive under a 90 min day/night cycle, clearing a potential obstacle for space experiments to grow cyanobacteria using ambient sunlight in LEO.

## 2. Materials and methods

### 2.1. Growth and culture conditions

Strains and plasmids are listed in Supplemental file, Table S1. *Escherichia coli* strains were grown in Lennox broth medium (LB) at 37 °C on agar plates or in glass test tubes rotated on a roller wheel with appropriate antibiotics (Table S2). Cyanobacterial culture and growth conditions were as previously described (Taton et al., 2014). Ten-mL samples of cyanobacterial strains were pre-cultured in BG-11 medium (Danchin et al., 1988) at 30 °C in 18 mm glass test tubes with shaking at 70–100 μmol photons $m^{-2}$ $s^{-1}$ constant white light. Light measurements were made with a QSL2100 PAR Scalar Irradiance sensor that measures photosynthetically active light from all directions (Biospherical Instruments, San Diego, CA).

For growth and competition assays, cyanobacteria were grown in time-, temperature-, and light-controlled incubators I-22LLX (Geneva Scientific). Cyanobacterial strains *Anabaena* PCC 7120, *Leptolyngbya* BL0902, and *Synechococcus elongatus* PCC 7942 were grown in 24-well plates in 1.2 mL/well BG-11 medium at 30 °C. Every 24 h fresh medium was added to account for evaporation and the cultures were mixed by manual bubbling with a multichannel pipet. The optical density at 750 nm ($OD_{750}$) was measured directly from the 24-well plates with a Tecan Infinite M200 plate reader.

Green algal strains *Scenedesmus dimorphus* UTEX1237 (*Scenedesmus*), *Chlamydomonas reinhardtii* CC-5082 (*Chlamydomonas*), and *Chlorella vulgaris* UTEX395 (*Chlorella*) were grown as described for cyanobacteria but in HSM medium (Schoepp 2014). Green algal culture growth was measured by fluorescence using a Tecan Infinite M200 plate reader with excitation of 485 nm and emission of 670 nm.

### 2.2. Circadian entrainment & analysis

Cyanobacterial strains AMC541 and AMC704 were pre-cultured for two days at 30 °C with shaking in glass test tubes, then standardized to a density of $OD_{750}$ = 0.2 with a Genesys 20 spectrophotometer (Thermo Fisher). Luciferase assays were prepared in 96-well plates (Tecan) (Paddock et al., 2013). Duplicate plates were initially entrained in opposite 12 h:12 h LD cycles in separate incubators with programmed lighting, then transferred to a Tecan Spark plate reader for measuring bioluminescence (Tecan). Plates were illuminated by white LED strip lights at 35 μmol photons $m^{-2}$ $s^{-1}$ with continuous light, or 70 μmol photons $m^{-2}$ $s^{-1}$ in LD cycles of 45′:45′ or 12 h:12 h. Bioluminescence from samples was measured every 90 min for 7 days. Values from edge wells were discarded due to desiccation risk (Paddock et al., 2013) and bioluminescence measurements were analyzed using BioDare2 software (Zielinski et al., 2014). Data were subjected to linear detrending and period length was calculated using FFT NLLS (Zielinski et al., 2014). Due to an unknown instrument error, in Fig. 2B every 16th data point was abnormally high, and was removed from the plot; the original plots are provided in Supplemental file, Fig. S1.

### 2.3. RB-TnSeq library experiment and insertion-site sequencing

We used quantitative sequencing of a characterized randomly barcoded transposon insertion sites (RB-TnSeq) library to screen for genes that affect the fitness of *S. elongatus* in 45′:45′ LD (Rubin et al., 2015). Cultures of the *S. elongatus* RB-TnSeq library were prepared as described previously (Rubin et al., 2015) from an aliquot archived at −80 °C. Cultures were grown in quadruplicate 50-mL volumes in plastic 250-mL tissue culture flasks (Falcon) bubbled with air at a rate of 2–3 bubbles/*sec*. Samples were taken prior to the start of the experiment ($T_0$) and at the end of 6 generations, as determined by $OD_{750}$ measurement of culture density. Barcode sequencing and analyses were conducted as described by Rubin et al. (Rubin et al., 2015). Raw barcode data mapped to the *S. elongatus* genome are available in Supplemental Dataset Tab S1.

### 2.4. Strain construction

For the construction of *S. elongatus* mutants, mapped single-gene transposon insertion mutants were selected from the *S. elongatus* Unigene set (UGS) (Holtman et al., 2005; Chen et al., 2012). Five-mL cultures of *E. coli* clones (Tables S1, S2) were grown in LB with appropriate antibiotics overnight, and plasmid DNA was extracted using a QIAprep Spin Miniprep Kit (Qiagen). To obtain insertion mutants, plasmid DNA was introduced into the *S. elongatus* chromosome by homologous recombination using natural transformation (Clerico et al., 2007). The presence and complete segregation of transposon insertions at each locus was verified by PCR.

For the complementation of *pgI* and *zwf* mutant strains, endogenous wild-type (WT) genes were PCR amplified from *S. elongatus* genomic DNA with primers listed in Table S3 using Q5 polymerase (NEB). Cloning vector pAM5433 targeting *S. elongatus* neutral site 3 was digested with SwaI (NEB), and plasmids (Table S1) were assembled using an Invitrogen Seamless Assembly kit (Invitrogen). Cloned genes were sequence verified by Sanger sequencing (GENEWIZ, San Diego, CA).

### 2.5. Competition assays & flow cytometry

Insertion-mutant strains marked with fluorescent reporter genes were generated by natural transformation of the mutant strain with either plasmid pAM5623 (mVenus) or pAM5634 (mTagBFP) (Table S1). Strains were verified by PCR. Knockout mutant and WT strains expressing either mVenus or mTagBFP reporter genes were pre-cultured in 5 mL of BG-11 for two days at 30 °C in 13 mm glass test tubes with shaking, then standardized to a density of $OD_{750}$ = 0.05 with a Genesys 20 spectrophotometer. Mutant strains carrying mVenus were mixed 1:1 with a WT strain carrying mTagBFP, and then analyzed with a CytoFLEX cell counter (Beckman Coulter) on days 0, 4, and 7. The experiment also included fluorophore-swapped strains as a control. Data were analyzed using CytExpert software (Beckman Coulter). Cytometer FSC and SSC gain were manually set to 1000, with a primary FSC threshold of 100,000 and secondary SSC threshold of 20,000. Viable *S. elongatus* cells were gated using cyanobacterial autofluorescence in the APC-A channel (gain 600), and of those, mVenus-positive or mTagBFP-positive cells were determined using FITC (gain 77) and PB450 (gain 41) channels. Due to cell aggregation, a small number of mVenus- and mTagBFP-positive cells were detected as doublets.

## 3. Results & discussion

### 3.1. Growth of cyanobacteria and green algae in 45′:45′ LD

We selected three lab-cultivated strains of cyanobacteria with diverse characteristics to test growth under conditions that mimic the LD cycle of LEO: *S. elongatus* PCC 7942, *Anabaena* PCC 7120 (hereafter *Anabaena*), and *Leptolyngbya* BL0902 (hereafter *Leptolyngbya*). *S. elongatus* is a unicellular model strain used for the study of many biological processes including its internal molecular circadian clock (Cohen and Golden, 2015). *Anabaena* is a multicellular, filamentous cyanobacterium that makes nitrogen-fixing heterocyst cells (Kumar et al., 2010). *Leptolyngbya* is a filamentous strain that does not make differentiated cell types and has characteristics suitable for bioproduction applications (Taton et al., 2012). All three strains are genetically tractable with established genetic methods and tools for genome engineering. *S. elongatus* is naturally transformable, capable of taking up and incorporating environmental DNA by homologous recombination into its genome at specific locations, which makes its genetics particularly straightforward (Taton et al., 2020).

*S. elongatus, Anabaena*, and *Leptolyngbya* were grown under three light conditions: continuous light at 75 μmol photons $m^{-2}$ $s^{-1}$; 45′:45′ LD cycles at 150 μmol photons $m^{-2}$ $s^{-1}$; and 12 h:12 h LD cycles at 150 μmol photons $m^{-2}$ $s^{-1}$. Despite providing the same photon flux over a 24 h period, the different lighting regimens had a noticeable effect on the growth rate of all three cyanobacterial strains (Fig. 1A). Each strain grew the fastest when supplied with continuous light and grew the slowest in 12 h:12 h LD. All three cyanobacterial strains grew faster in 45′:45′ LD compared to standard 12 h:12 h LD. The mechanisms that contribute to faster growth in 45′:45′ LD are not known.

We also examined how unicellular green algae, which are eukaryotic photosynthetic microorganisms, would grow in 45′:45′ LD. Some strains of green algae are genetically

tractable, and can express bioactive recombinant proteins, as well as biofuel molecules and plastic precursors (Rasala and Mayfield, 2015; Scranton et al., 2015; Phung Hai et al., 2020). Several strains of green algae are edible, including *Chlamydomonas reinhardtii*, which was recently shown to help improve gut microbiome health (Fields et al., 2020). We used three green algal strains: *Chlamydomonas reinhardtii, Chlorella vulgaris*, and *Scenedesmus dimorphus*. While the green algae grew fastest in continuous light, their growth rates were nearly the same in 12 h:12 h LD and 45′:45′ LD (Fig. 1B). Unlike the cyanobacterial strains, the algal strains did not grow faster in 45′:45′ LD compared to 12 h:12 h LD. These results indicate basic differences in metabolism or in managing the dark/light transition between these prokaryotic and eukaryotic photosynthetic microorganisms. Importantly, all strains of green algae and cyanobacteria tested grew well under continuous light and a 45′:45′ LD regime, demonstrating a wide range of light period tolerances.

### 3.2. The circadian clock is not impacted by 45′:45′ LD

We monitored the circadian rhythms of gene expression in *S. elongatus* grown in 45′:45′ LD using the bioluminescent reporter strain AMC541, in which the *luc* gene encoding luciferase is driven by the *kaiBC* promoter. When provided with luciferin substrate, light production oscillates as a function of gene expression, which is under the control of the circadian clock (Markson et al., 2013). The internal clock can be synchronized to environmental light-dark periods and then the 24 h circadian oscillation of the biological clock will continue to run and regulate cellular activities in the absence of LD cycle inputs. When released from LD entrainment and placed in continuous light conditions, the clock maintains a “free-running” period of slightly more than 24 h (Ouyang, 1998).

*S. elongatus* AMC541 cultures were first entrained in 12 h:12 h LD to synchronize all the cells to a 24 h cycle with the same phase of peak bioluminescence (Cohen et al., 2018). The cells were entrained in 96-well agar plates for at least two dark periods in 12 h:12 h LD. Two plates were separately incubated with their entrainment offset by 11 h 15 min. This is 45 min short of a full 12 h opposite phase, so that each plate would be in the light during sampling. Using plates in nearly opposite phase allowed us to test the effect of changing from a 24 h LD cycle to a 90 min LD cycle at two important time points: the expected dark-to-light transition (dawn, plate 1), and the expected light-to-dark transition (dusk, plate 2). This strategy was used because cells might exhibit different responses or tolerances to 45′:45′ LD depending on the phase of the clock when the change occurs. After entrainment, both 96-well plates were moved at the same time to a 45′:45′ LD lighting condition and bioluminescence was measured every 90 min for 7 days. Plate 1 was transitioned to 45′:45′ LD near its subjective dawn (as determined by the internal circadian clock), such that it received an extra 45 min of darkness, and plate 2 was transitioned near its subjective dusk, such that it received 45 min less light during its light phase.

For control experiments, oppositely entrained plates were moved to either standard 12 h:12 h LD or continuous light, and bioluminescence was monitored for 7 days (Fig. 2B,C). The experimental data show that a short 45′:45′ LD cycle had a similar effect to transferring the cells into constant light; the phase of the internal circadian rhythm did not shift from the entrainment conditions (Fig. 2A,C). However, a long dark exposure (12 h) reset the clock

so that cells were shifted to the new LD cycle (Fig. 2B). These results were not unexpected because 45 min of darkness is known to be too short a duration of darkness to cause a phase shift of the internal clock; a dark pulse of 5 h is routinely used to reliably reset the clock in *S. elongatus* (Schmitz et al., 2000).

The circadian periods of bioluminescence from the reporter strains were analyzed using BioDARE2 software (Zielinski et al., 2014). Growth in 45′:45′ LD, whether started at subjective dawn or subjective dusk for cells entrained to 12 h:12 h LD, did not have an impact on the circadian period of gene expression, which remained constant at just over 24 h. The experiment was also run with the "clockless" mutant strain AMC704, in which the *kaiC* gene has been deleted to provide a non-rhythmic control (Paddock et al., 2013). This control strain displayed no inherent rhythmic reporter signal and showed little difference between the two plates (data not shown).

### 3.3. Random-barcode transposon insertion-site sequencing for growth in 45′:45′ LD

We used a randomly barcoded transposon insertion-site sequencing (RB-TnSeq) mutant library in *S. elongatus* (Rubin et al., 2015) to identify genes whose knockout mutants affects the fitness of *S. elongatus* in 45′:45′ LD. The RB-TnSeq library contains clones of cells with single transposon insertions at different random locations in the genome. Each transposon contains a unique 20-bp DNA sequence tag called a "barcode", and the transposon position in the genome and the associated barcode sequence for each mutant in the library was previously determined by deep sequencing (Rubin et al., 2015). The RB-TnSeq library comprises approximately 250,000 unique mutant strains, representing an insertion roughly every 11 bp in nearly all nonessential genes of the 2.7-Mbp *S. elongatus* genome. The RB-TnSeq library was initially used by Rubin et al. to determine that 764 of 2723 *S. elongatus* genes are essential for cell survival during photoautotrophic growth (Rubin et al., 2015). RB-TnSeq libraries can be used to quantitatively determine the fitness value of every non-essential gene under a variety of selective pressures (Price et al., 2018). After growth of the library under selective conditions, all barcodes in the sample are amplified by PCR and identified quantitatively by sequencing to determine the prevalence of each barcoded mutant in the surviving population.

RB-TnSeq experiments with *S. elongatus* have been performed for many different growth conditions, including LD cycles, temperature, osmotic stress, and antibiotic resistance (Price et al., 2018). The data from these experiments have been used to generate a database of conditional fitness effects, allowing us to determine gene cofitness, a measurement of how well gene fitness patterns correlate between different selective growth conditions (Price et al., 2018).

For our experiments, an aliquot of the *S. elongatus* RB-TnSeq library was thawed and grown for six generations under two conditions: standard 12 h:12 h LD for the control conditions and 45′:45′ LD to simulate conditions in LEO (Fig. 3A). As was true for WT *S. elongatus*, the RB-TnSeq library grew nearly twice as fast in 45′:45′ LD as in 12 h:12 h LD (Fig. 3B). To minimize self-shading and keep the cells actively dividing, cultures were diluted when the $OD_{750}$ exceeded 0.5. After six generations of growth, genomic DNA was extracted from

the cells, library barcodes were PCR amplified and sequenced, and quantitative analyses of gene fitness were performed (Rubin et al., 2015).

Pair-wise analyses of the RB-TnSeq data produces a fitness value for each gene and the log of the false discovery rate (log_fdr), which functions as a *p*-value (Price et al., 2018). The analysis of the RB-TnSeq control data from 12 h:12 h LD growth conditions compared with the data from 45′:45′ LD is represented in Fig. 3A as the difference in fitness between **a** and **b**. This analysis identifies mutants with different fitness between 12 h:12 h LD and 45′:45′ LD (Supplemental Dataset Tab S2). However, we found that the gene fitness effects of 45′:45′ LD were being masked by the greater magnitude of the fitness changes observed in 12 h:12 h LD.

To separate these fitness effects, we focused our analysis on gene fitness between the starting timepoint ($T_0$) and the ending timepoint in 45′:45′ LD, represented by dotted line **b** in Fig. 3A. This $T_0$ analysis compares the difference between gene prevalence at $T_0$, which represents the RB-TnSeq library grown under continuous light, and the end point, after 6 generations of growth in 45′:45′ LD (Fig. 3C, Table 1, Supplemental Dataset Tab S3).

We examined genes whose transposon mutation resulted in an absolute fitness score > 2; i.e., those with strong, definitive phenotypes (Price et al., 2018). Comparing fitness under 45′:45′ LD to the $T_0$ sample grown in continuous light, there were only 38 genes whose loss conferred a positive fitness, and all of these had a fitness score under 0.5, well below the threshold for a definitive phenotype (Supplemental Dataset Tab S3). Genes whose loss negatively impact fitness identify cell functions or pathways that are important for survival in 45′:45′ LD. Five genes with a fitness score below −2 merited further analysis, in part because they all have a high degree of cofitness from prior RB-TnSeq experiments (Fig. 3D) (Price et al., 2018). These five genes play an important role in *S. elongatus* dark metabolism, glycogen degradation, and the oxidative pentose phosphate pathway (OPPP), which are crucial to surviving the 12-h dark period of night (Diamond et al., 2017; Welkie et al., 2018). In a screen of the RB-TnSeq library, Welkie et al. identified that the loss of each of these genes resulted in a strong fitness decrease in 12 h:12 h LD compared to continuous light (Welkie et al., 2018). In addition to providing the cells energy in the dark by metabolizing glycogen, the OPPP is necessary during long dark periods to clear reactive oxygen species (ROS) that accumulate during the light period. OPPP mutants have no growth defect in continuous light because sufficient energy and reductant are provided by photosynthesis to avoid ROS damage. The most unfit mutant in 12 h:12 h LD had insertions in *kaiA*, a key component of the circadian clock whose loss renders cells unable to activate the OPPP at dusk. In our 45′:45′ LD experiment, the loss of *kaiA* had only a slight negative fitness score (Table 1), well below the threshold for even weak phenotypes. Altogether, our results suggest that in short 45′:45′ LD cycles, the cells are not accumulating toxic levels of ROS that require clock-controlled activation of dusk genes to remove. Nevertheless, inactivation of the OPPP genes is partially detrimental to growth in 45′:45′ LD, presumably because the cells need an energy source during the 45 min dark periods to maintain cellular growth functions and provide Calvin-Benson-Bassham (CBB) cycle intermediates (Shinde et al., 2020).

### 3.4. Validation of mutant phenotypes

To validate and further characterize the mutants identified in the RB-TnSeq screen, we focused on five mutants in the OPPP, which provides energy to cells in darkness by metabolizing glycogen, the primary energy storage molecule of the cells (Fig. 3F). Most of the genes in the *S. elongatus* OPPP are essential for survival under standard growth conditions, and therefore those mutants are not represented in the library (Rubin et al., 2015). The five genes we identified are not essential when cells are grown in continuous light, but strains with mutations in these non-essential OPPP genes have reduced fitness when exposed to long dark periods because the OPPP produces reductant required for dark survival (Diamond et al., 2017; Welkie et al., 2018). To determine the effect of defects in the OPPP and glycogen metabolism on cells in 45′:45′ LD growth conditions, we generated insertion mutants of the genes *pgI* (Synpcc7942_0529), *zwf* (Synpcc7942_2334), *opcA* (Synpcc7942_2333), *tal* (Synpcc7942_2297), and *glgP* (Synpcc7942_0244). Independent colonies were selected to obtain triplicate mutant strains in a WT background as well as in fluorescent reporter backgrounds that express yellow fluorescent protein (mVenus) or a blue fluorescent protein (mTagBFP). These reporter strains can be distinguished from each other by flow cytometry and the proportion of each strain in a mixed culture can be monitored during growth competition experiments to compare the relative fitness of different mutants.

Growth competition assays can determine even small differences in the relative fitness of different genotypes. The RB-TnSeq library subjects hundreds of thousands of different mutant strains to competition against each other to determine their fitness under different environmental conditions. Small effects that might not be measurable if a mutant strain were grown alone are amplified when strains compete for resources (Welkie et al., 2018). We performed growth competition experiments with WT against each of the five OPPP and glycogen metabolism mutants and, as a control, a mutant of an unrelated uncharacterized gene (Synpcc7942_2380) that had a neutral fitness value from the RB-TnSeq results (Table 1). For each gene, WT background cells with mTagBFP, WT(mTagBFP), were mixed with mutant background cells that carried the mVenus reporter, mutant(mVenus) (Table S1), and grown in both continuous light and 45′:45′ LD conditions for 7 days (Fig. 4A).

We measured the concentrations of mTagBFP or mVenus cells in the mixed cultures over time using flow cytometry. For example, starting from a nearly even mix of mutant and WT cells at day 0, the *pgI* mutant strain dropped to a tiny fraction of the total population by day 7 (Fig. 4B). The other OPPP mutants had very similar outcomes in competition against WT in 45′:45′ LD, each dropping to less than 3% of the total population after a week of growth, while the control Synpcc7942_2380 mutant maintained its relative population level throughout the experiment (Fig. 4C). Under continuous light conditions, the mutant strains grew similarly to each other and maintained population levels similar to WT, with only minor differences in their relative ratios (Fig. 4D). In parallel, we made control strains in which the fluorescent reporters were swapped, resulting in WT(mVenus) and mutant (mTagBFP), and we obtained similar data for these reporter-swap experiments (Fig. S2). Swapping the fluorescent reporters was performed to control for potential differential impacts on growth rate caused by expression of the different fluorescent reporters. These data demonstrate that the OPPP and glycogen metabolism mutants are rapidly outcompeted

by WT cells when grown with periods of darkness and validate the fitness data generated by the RB-TnSeq experiment for these mutants.

### 3.5. Growth rate comparison and complementation of mutant phenotypes

We grew the different OPPP and glycogen metabolism mutant strains under continuous light and 45′:45′ LD and measured their growth to clarify why the mutant strains had lower fitness levels under 45′:45′ LD. Because the continuous-light cultures grew more quickly, those cultures were diluted with fresh medium on day 4 to minimize self-shading and keep them actively dividing. In continuous light, the mutant strains showed no growth defects and grew as well as WT (Fig. 5A). Minor differences in the growth curves reflect slight variations in the initial concentration of each culture, and were consistent throughout the course of the experiment. In 45′:45′ LD, however, each of the mutant strains grew more slowly than WT, with *zwf* growing slowest and reaching only about one-third the culture density of WT after a week (Fig. 5B). These growth defects are consistent with the results from the competition experiments because mutant cells that divide more slowly will be quickly overgrown by WT. The growth rates of the mutants roughly correlated with their relative fitness in the competition experiments. For example, *zwf* and *tal* had the lowest relative fitness of the mutants in the competition experiments, and likewise had the slowest growth rates. The differences in growth rates between the mutant strains may be due to altered regulation or the presence of alternative metabolic intermediates. For example, the *glgP* mutant grew faster than the *zwf* mutant, possibly because the cells have ways of generating glucose-6-phosphate other than glycolysis, such as processing from fructose-6-phosphate (Fig. 3E).

We selected two mutants, *zwf* and *pgI,* to complement with WT alleles to confirm that the slower growth rate was linked directly to the knockout of the OPPP genes and not to second-site mutations. The complementing genes were cloned into *S. elongatus* neutral site 3, a location in the genome where DNA insertions have no obvious secondary effects (Clerico et al., 2007). Each gene was driven by a P*trc* promoter, which is inducible with IPTG, but has a low level of “leaky” uninduced expression. In this case, the leaky expression was sufficient to rescue the growth defect phenotype of the mutant strains. Both *zwf*- and *pgI*-complemented strains grew as well as WT in 45′:45′ LD while the knockout strains grew more slowly (Fig. 5D). Growth in continuous light was similar for all strains (Fig. 5C).

To determine whether the fitness effects were due to slower growth or cell death, we performed cell viability assays by fluorescence and light microscopy. The autofluorescence of cyanobacterial photosynthetic pigments can be used to measure cell viability because dead cells remain visible via light microscopy but lose autofluorescence shortly after death (Kawasaki and Iwasaki, 2020; Schulze et al., 2011). On days one and three, we took microscopic images of cell fields for each mutant and the complemented strains grown under continuous light and 45′:45′ LD. Then we calculated the percentage of cells that were viable (Fig. 5E). There was no difference in cell mortality between continuous light and 45′:45′ LD, which indicates that cells in 45′:45′ LD grow more slowly than in continuous light but do not die. These results are in contrast to some OPPP mutants grown in a 12 h:12 h LD cycle, which accumulate reactive oxygen species during the 12 h light period and fail

to clear them after onset of darkness, causing the cells to die after a few hours (Diamond et al., 2017).

## 4. Conclusions

In these experiments, we demonstrated that the 45 min day and 45 min night of LEO provides a suitable light environment for the growth of green algae and cyanobacteria. The 45 min LD cycle appears to be too short a time to disrupt the rhythms of the cyanobacterial circadian clock that evolved in a 24 h day (Schmitz et al., 2000). Unexpectedly, all the WT cyanobacterial strains grew better in 45′:45′ LD than in 12 h:12 h LD. An explanation for this result may be that in *S. elongatus*, light availability drives metabolism (Pattanayak et al., 2015). *S. elongatus* stops replicating DNA and dividing at night, but in 45′:45′ LD, with light energy restarting metabolism every 45 min, the cells may never experience an energy deficit severe enough to suspend metabolic processes as would normally occur at night. Green algae, like cyanobacteria, utilize circadian rhythms to regulate their metabolism, and may sense multiple environmental cues to appropriately set their circadian clocks (Pattanayak et al., 2015; Petersen et al., 2022; Matsuo and Ishiura, 2011). Green algal strains did not grow more quickly in 45′:45′ LD than 12 h:12 h LD, and this may be due to the more complex environmental-sensing mechanisms in eukaryotic microalgae compared to cyanobacteria, in which light is perceived mainly by its impact on photosynthetic metabolic activity.

Another important finding is that cellular energy storage and retrieval pathways such as the OPPP and glycogen metabolism are important for continuous growth during short periods of darkness. Previous research has shown that glycogen metabolism and the OPPP are critical during the dark/light transition to jump-start photosynthesis by increasing NADPH levels (Shinde et al., 2020). In our experiments, the growth characteristics of the OPPP mutants support that hypothesis, and suggest that 45 min of darkness is enough to deplete cellular NADPH levels. The viability of OPPP mutants in 45′:45′ LD, and the lack of an apparent growth defect for a *kaiA* mutant in the RB-TnSeq screen, suggest that the LEO light exposure regimen does not generate high levels of ROS during the light period that are toxic for the cells. Taken together, our data presented here show that the length of light and dark periods is an important factor to consider for cyanobacterial growth, even in unusual regimes like 45′:45′ LD.

Light exposure will be an important consideration when utilizing cyanobacteria in a BLS system in the space environment. Electric lighting elements have high energy costs and limited lifetimes; a growth system that is able to use ambient sunlight can save both energy and design complexity costs. Despite some suggestions to the contrary (Keller et al., 2021), cyanobacteria do not need a dark period to survive and in fact grow more quickly in continuous light. For space journeys outside of Earth's orbit, or in the lunar polar region, sunlight is nearly constant. LEO, the location of the ISS and planned future space stations, is suitable to test cyanobacteria-based BLS systems using ambient sunlight, since its unusual 45′:45′ LD period is no obstacle to growth. While there may exist challenges to scaling up cyanobacterial cultivation to suitable volumes for space missions that affect gas exchange of oxygen and $CO_2$ or other growth parameters, the biological clock in cyanobacteria is

proven to be remarkably robust and resilient to different growth conditions and genetic backgrounds, and therefore we expect that the effects of a 45′:45′ LD cycle are unlikely to change at larger growth scales.

Cyanobacteria are among the simplest and most efficient organisms capable of removing carbon dioxide, replenishing oxygen, and producing biomass. Cyanobacteria are typically grown in liquid cultures where the cells in suspension are in constant Brownian motion that mimics a weightless environment. Microgravity appears not to be an impediment to their growth as demonstrated by Poughon et al. for *Limnospira indica* (Poughon et al., 2020). The entire cyanobacterial cell is photosynthetic, providing an efficiency advantage over plants that must grow secondary structures such as roots and vasculature. Cyanobacteria and other microalgae can also be cultivated using ammonium and urea from urine, another useful component of BLSS, and several strains are edible (Hendrickx et al., 2006; Fields et al., 2020; Canizales et al., 2021). With short generation times, small genomes, and robust genetic tools like those used in this work, cyanobacteria are excellent candidate organisms for investigating bacterial adaptation to a space environment in support of human exploration.

## Supplementary Material

Refer to Web version on PubMed Central for supplementary material.

## Acknowledgments

We acknowledge Dustin Ernst for providing the fluorophore-labeled plasmids pAM5623 and pAM5634, and Arnaud Taton and Marie Adomako for assistance in manuscript editing. Funding was made available by the National Aeronautics and Space Administration (NASA) Space Biology Program grant number 80NSSC19K0136. Research reported in this publication was supported in part by the National Institute of General Medical Sciences of the National Institutes of Health under Award Number R35GM118290 (to SSG). The content is solely the responsibility of the authors and does not necessarily represent the official views of the National Institutes of Health. This material is also based in part upon work supported by the National Science Foundation under Grant number IOS-1754946 (to JWG). Any opinions, findings, and conclusions or recommendations expressed in this material are those of the author(s) and do not necessarily reflect the views of the National Science Foundation.

## References

Canizales S, Sliwszcinka M, Russo A, Bentvelzen S, Temmink H, Verschoor AM, et al. , 2021. Cyanobacterial growth and cyanophycin production with urea and ammonium as nitrogen source. J. Appl. Phycol. 33, 3565–3577. 10.1007/s10811-021-02575-0.

Chen Y, Holtman CK, Taton A, Golden SS, 2012. Functional analysis of the Synechococcus elongatus PCC 7942 genome. Adv. Photosynth. Respir. 119–137. 10.1007/978-94-007-1533-2_5.

Clerico EM, Ditty JL, Golden SS Specialized techniques for site-directed mutagenesis in cyanobacteria 2007:155–71. 10.1007/978-1-59745-257-1_11.

Cohen SE, Golden SS, 2015. Circadian rhythms in cyanobacteria. Microbiol. Mol. Biol. Rev. 10.1128/mmbr.00036-15.

Cohen SE, McKnight BM, Golden SS, 2018. Roles for ClpXP in regulating the circadian clock in Synechococcus elongatus. Proc. Natl. Acad. Sci. U. S. A. 115, E7805–E7813. 10.1073/pnas.1800828115. [PubMed: 30061418]

Cottin H, Rettberg P, 2019. EXPOSE-R2 on the international space station (2014–2016): results from the PSS and BOSS astrobiology experiments. Astrobiology 19, 975–978. 10.1089/ast.2019.0625. [PubMed: 31373529]

Danchin A, Haddox MK, Whitton BA, Van Baalen C, Tabita FR, Rippka R, et al. Harvesting of cells. 1988;167:584–91.

De Vera J, Alawi M, Backhaus T, Baque M, Billi D, Bo U, et al. Limits of life and the habitability of mars : the ESA space experiment BIOMEX on the ISS 2019;19:145–57. 10.1089/ast.2018.1897.

Diamond S, Rubin BE, Shultzaberger RK, Chen Y, Barber CD, Golden SS, 2017. Redox crisis underlies conditional light–dark lethality in cyanobacterial mutants that lack the circadian regulator, RpaA. Proc. Natl. Acad. Sci. 114, E580–E589. 10.1073/pnas.1613078114. [PubMed: 28074036]

Fields FJ, Lejzerowicz F, Schroeder D, Ngoi SM, Tran M, McDonald D, et al. , 2020. Effects of the microalgae Chlamydomonas on gastrointestinal health. J. Funct. Foods 65, 103738. 10.1016/j.jff.2019.103738.

Golden SS, 2020. Principles of rhythmicity emerging from cyanobacteria. Eur. J. Neurosci. 51, 13–18. 10.1111/ejn.14434. [PubMed: 31087440]

Hendrickx L, De Wever H, Hermans V, Mastroleo F, Morin N, Wilmotte A, et al. , 2006. Microbial ecology of the closed artificial ecosystem MELiSSA (Micro-ecological life support system alternative): reinventing and compartmentalizing the Earth's food and oxygen regeneration system for long-haul space exploration missions. Res. Microbiol. 157, 77–86. 10.1016/j.resmic.2005.06.014. [PubMed: 16431089]

Holtman CK, Chen Y, Sandoval P, Gonzales A, Nalty MS, Thomas TL, et al. , 2005. High-throughput functional analysis of the Synechococcus elongatus PCC 7942 genome. DNA Res. 10.1093/dnares/12.2.103.

Inoue K, Araki T, Endo M, 2018. Circadian clock during plant development. J. Plant Res. 131, 59–66. 10.1007/s10265-017-0991-8. [PubMed: 29134443]

Ishiura M, Kutsuna S, Aoki S, Iwasaki H, Andersson CR, Tanabe A, et al. , 1998. Expression of a gene cluster kaiABC as a circadian feedback process in cyanobacteria. Science 281, 1519–1523. 10.1126/science.281.5382.1519, 80-. [PubMed: 9727980]

Kawasaki K, Iwasaki H, 2020. Involvement of glycogen metabolism in circadian control of UV resistance in cyanobacteria. PLOS Genet. 16, e1009230 10.1371/journal.pgen.1009230. [PubMed: 33253146]

Keller RJ, Porter W, Goli K, Rosenthal R, Butler N, Jones JA, 2021. Biologically-based and physiochemical life support and in situ resource utilization for exploration of the solar system —reviewing the current state and defining future development needs. Life 11, 844. 10.3390/life11080844. [PubMed: 34440588]

Kumar K, Mella-Herrera RA, Golden JW, 2010. Cyanobacterial heterocysts. Cold Spring Harb. Perspect. Biol. 2 10.1101/cshperspect.a000315.

Markson JS, Piechura JR, Puszynska AM, O'Shea EK, 2013. Circadian control of global gene expression by the cyanobacterial master regulator RpaA. Cell 155, 1396–1408. 10.1016/j.cell.2013.11.005. [PubMed: 24315105]

Martin W, Kowallik K, 1999. Annotated english translation of mereschkowsky's 1905 paper 'Über natur und ursprung der chromatophoren impflanzenreiche.'. Eur. J. Phycol. 34, 287–295. 10.1080/09670269910001736342.

Matsuo T, Ishiura M, 2011. Chlamydomonas reinhardtii as a new model system for studying the molecular basis of the circadian clock. FEBS Lett. 585, 1495–1502. 10.1016/j.febslet.2011.02.025. [PubMed: 21354416]

Ode KL, Ueda HR, 2018. Design principles of phosphorylation-dependent timekeeping in eukaryotic circadian clocks. Cold Spring Harb. Perspect. Biol. 10 10.1101/cshperspect.a028357.

Ouyang Y, 1998. Resonating circadian clocks enhance fitness in cyanobacteria. Ecol. Modell. 95, 8660–8664. 10.1016/j.ecolmodel.2010.03.015.

Paddock ML, Boyd JS, Adin DM, Golden SS, 2013. Active output state of the Synechococcus Kai circadian oscillator. Proc. Natl. Acad. Sci. U. S. A. 110, 3849–3857. 10.1073/pnas.1315170110.

Pattanayak GK, Lambert G, Bernat K, Rust MJ, 2015. Controlling the cyanobacterial clock by synthetically rewiring metabolism. Cell Rep. 13, 2362–2367. 10.1016/j.celrep.2015.11.031. [PubMed: 26686627]

Petersen J, Rredhi A, Szyttenholm J, Mittag M, 2022. Evolution of circadian clocks along the green lineage. Plant Physiol. 924–937. 10.1093/plphys/kiac141.

Phung Hai TA, Neelakantan N, Tessman M, Sherman SD, Griffin G, Pomeroy R, et al. , 2020. Flexible polyurethanes, renewable fuels, and flavorings from a microalgae oil waste stream. Green Chem. 22, 3088–3094. 10.1039/d0gc00852d.

Poughon L, Laroche C, Creuly C, Dussap CG, Paille C, Lasseur C, et al. , 2020. Limnospira indica PCC8005 growth in photobioreactor: model and simulation of the ISS and ground experiments. Life Sci. Space Res. 25, 53–65. 10.1016/j.lssr.2020.03.002.

Price MN, Wetmore KM, Waters RJ, Callaghan M, Ray J, Liu H, et al. , 2018. Mutant phenotypes for thousands of bacterial genes of unknown function. Nature 557, 503–509. 10.1038/s41586-018-0124-0. [PubMed: 29769716]

Rasala BA, Mayfield SP, 2015. Photosynthetic biomanufacturing in green algae; production of recombinant proteins for industrial, nutritional, and medical uses. Photosynth. Res. 123, 227–239. 10.1007/s11120-014-9994-7. [PubMed: 24659086]

Rubin BE, Wetmore KM, Price MN, Diamond S, Shultzaberger RK, Lowe LC, et al. , 2015. The essential gene set of a photosynthetic organism. Proc. Natl. Acad. Sci. 112, E6634–E6643. 10.1073/pnas.1519220112. [PubMed: 26508635]

Schirrmeister BE, Gugger M, Donoghue PCJ, 2015. Cyanobacteria and the great oxidation event: evidence from genes and fossils. Palaeontology 58, 769–785. 10.1111/pala.12178. [PubMed: 26924853]

Schmitz O, Katayama M, Williams SB, Kondo T, Golden SS, 2000. CikA, a bacteriophytochrome that resets the cyanobacterial circadian clock. Science 289, 765–768. 10.1126/science.289.5480.765, 80-. [PubMed: 10926536]

Schulze K, López DA, Tillich UM, Frohme M, 2011. A simple viability analysis for unicellular cyanobacteria using a new autofluorescence assay, automated microscopy, and ImageJ. BMC Biotechnol. 11 10.1186/1472-6750-11-118.

Scranton MA, Ostrand JT, Fields FJ, Mayfield SP, 2015. Chlamydomonas as a model for biofuels and bio-products production. Plant J. 82, 523–531. 10.1111/tpj.12780. [PubMed: 25641390]

Shih PM, Wu D, Latifi A, Axen SD, Fewer DP, Talla E, et al. , 2013. Improving the coverage of the cyanobacterial phylum using diversity-driven genome sequencing. Proc. Natl. Acad. Sci. 110, 1053–1058. 10.1073/pnas.1217107110. [PubMed: 23277585]

Shinde S, Zhang X, Singapuri SP, Kalra I, Liu X, Morgan-Kiss RM, et al. , 2020. Glycogen metabolism supports photosynthesis start through the oxidative pentose phosphate pathway in cyanobacteria. Plant Physiol. 182, 507–517. 10.1104/pp.19.01184. [PubMed: 31649110]

Song W, Zhao C, Zhang D, Mu S, Pan X, 2016. Different resistance to UV-B radiation of extracellular polymeric substances of two cyanobacteria from contrasting habitats. Front. Microbiol. 7, 1–8. 10.3389/fmicb.2016.01208. [PubMed: 26834723]

Taton A, Erikson C, Yang Y, Rubin BE, Rifkin SA, Golden JW, et al. , 2020. The circadian clock and darkness control natural competence in cyanobacteria. Nat. Commun. 11, 1–11. 10.1038/s41467-020-15384-9. [PubMed: 31911652]

Taton A, Lis E, Adin DM, Dong G, Cookson S, Kay SA, et al. , 2012. Gene transfer in Leptolyngbya sp. strain BL0902, a cyanobacterium suitable for production of biomass and bioproducts. PLoS ONE 7, 1–15. 10.1371/journal.pone.0030901.

Taton A, Unglaub F, Wright NE, Zeng WY, Paz-Yepes J, Brahamsha B, et al. , 2014. Broad-host-range vector system for synthetic biology and biotechnology in cyanobacteria. Nucleic Acids Res. 42, 1–16. 10.1093/nar/gku673. [PubMed: 24376271]

Welkie DG, Rubin BE, Chang YG, Diamond S, Rifkin SA, LiWang A, et al. , 2018. Genome-wide fitness assessment during diurnal growth reveals an expanded role of the cyanobacterial circadian clock protein KaiA. Proc. Natl. Acad. Sci. U. S. A. 115, E7174–E7183. 10.1073/pnas.1802940115. [PubMed: 29991601]

Zielinski T, Moore AM, Troup E, Halliday KJ, Millar AJ, 2014. Strengths and limitations of period estimation methods for circadian data. PLoS ONE. 10.1371/journal.pone.0096462.

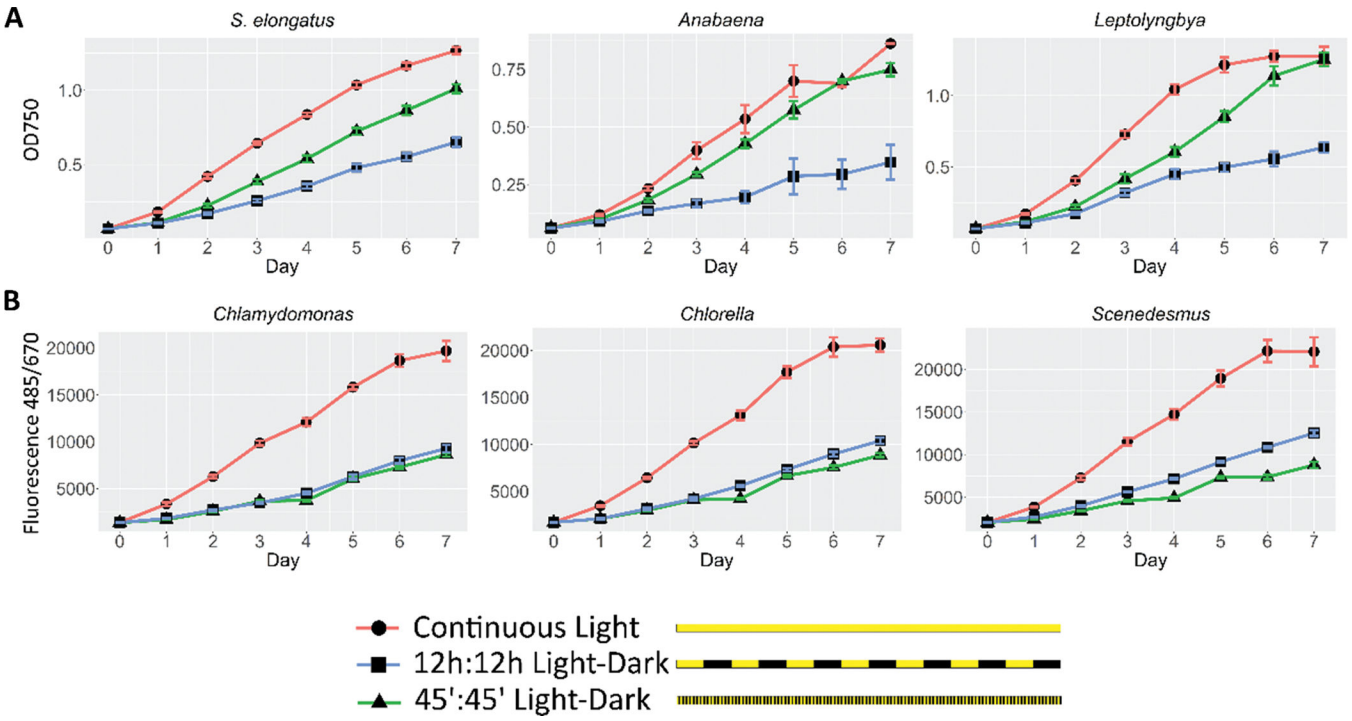


**Fig. 1.**

Growth of cyanobacteria and green algae under different light-dark conditions. (A) Cyanobacterial strains *S. elongatus, Anabaena*, and *Leptolyngbya* grown in continuous light, 45′:45′ LD, or 12 h:12 h LD. (B) Green algal strains *Chlamydomonas, Chlorella*, and *Scenedesmus* grown under the same conditions. Strains were grown in quadruplicate; error bars represent mean ± SEM.

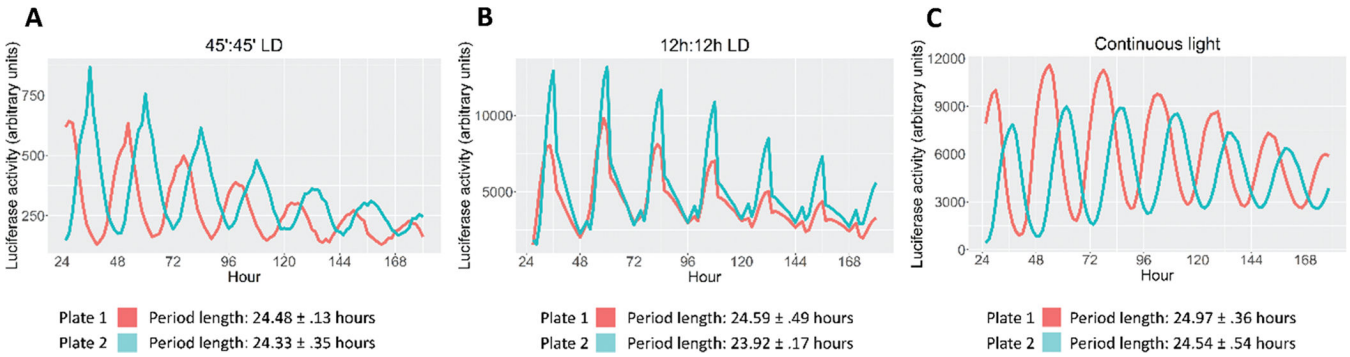


**Fig. 2.**

Circadian rhythms of *S. elongatus* in 45′:45′ LD. Circadian reporter strain AMC541 was entrained in separate 96-well plates to opposite phases of 12 h:12 h LD, then changed to (A) 45′:45′ LD, (B) 12 h:12 h LD, or (C) continuous light. Bioluminescence was measured over 7 days. BioDARE2 analysis of the free-running period is shown below each panel. The reporter strains maintain consistent circadian rhythms for weeks in the absence of external lighting cues; however, the amplitude of the bioluminescence signal damped over time in all samples.

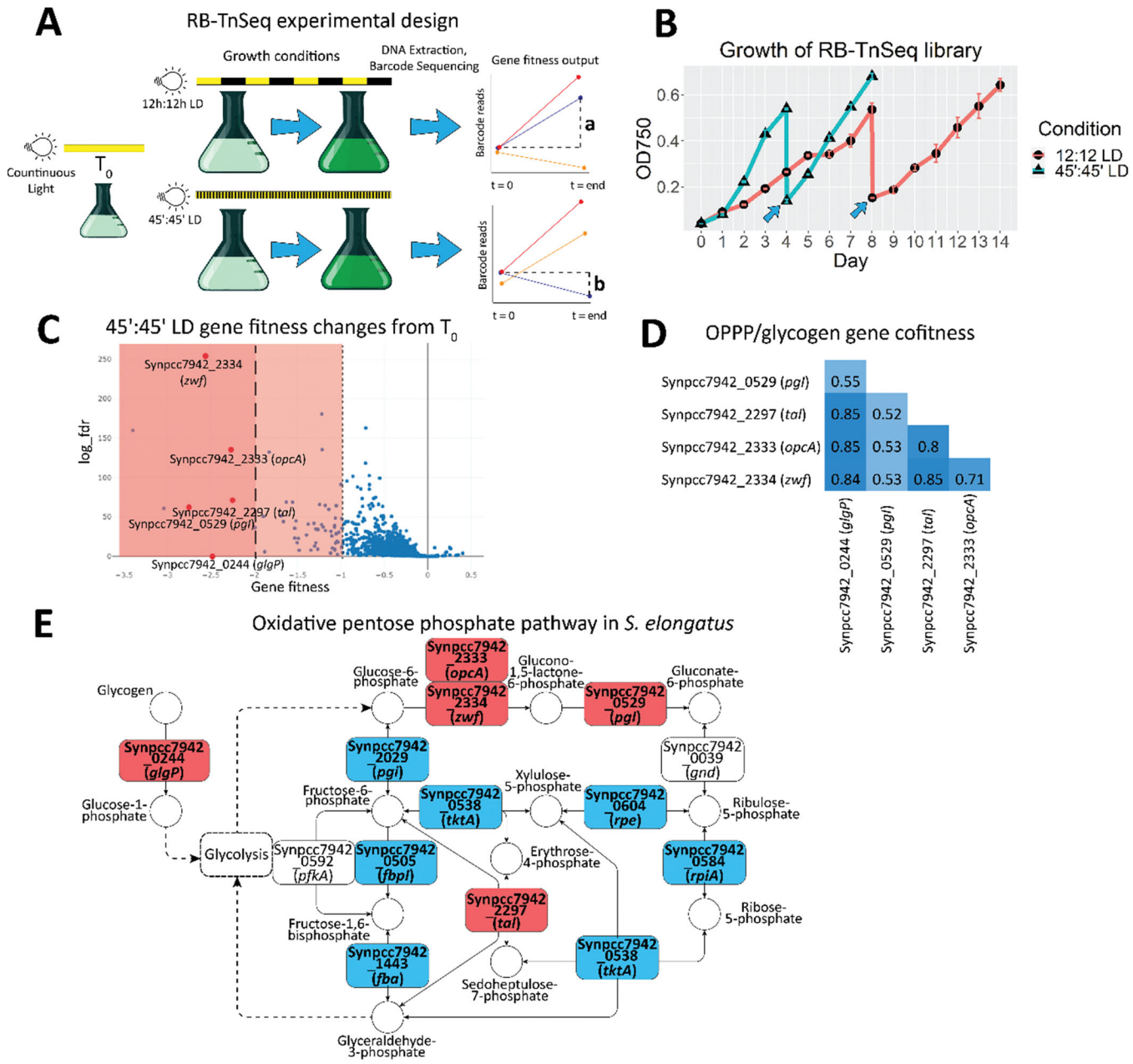


**Fig. 3.**

RB-TnSeq experiment of *S. elongatus* 45′:45′ LD growth. (A) Experimental design of the RB-TnSeq experiment. Graphs show potential results for 3 hypothetical genes. (B) Growth rates of the RB-TnSeq library over 6 generations. Cultures were diluted on days 4 and 8, respectively (blue arrows). (C) Volcano plot of $T_0$ analysis of fitness values (x-axis) against the log_fdr for 45′:45′ LD vs. continuous light. Dark and light red shading represent thresholds for strong and weaker phenotypes, respectively. Red dots indicate genes with high cofitness values (D) and that are part of the *S. elongatus* oxidative pentose phosphate pathway (OPPP) shown in (E). Genes in light red are among those whose loss generates the most negative fitness values in the $T_0$ analysis; genes in light blue are essential for survival

under standard growth conditions and those mutants are not represented in the RB-TnSeq library.

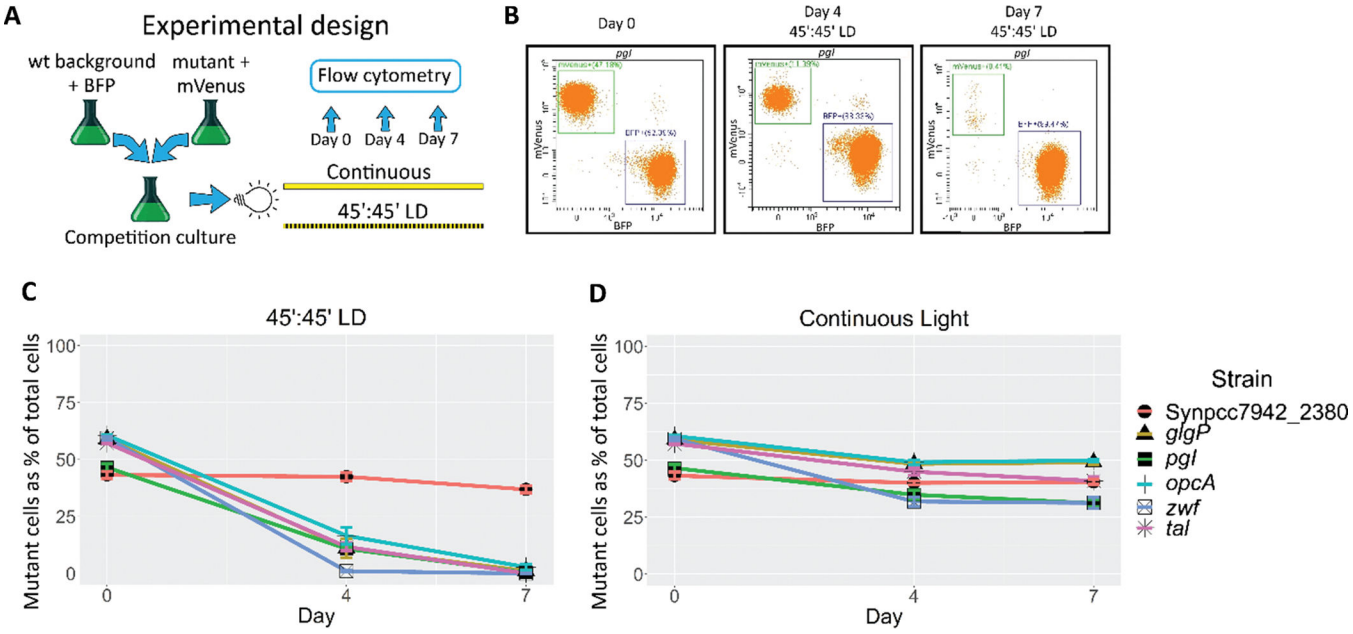


**Fig. 4.**

Growth competition analysis of OPPP and glycogen metabolism mutants. (A) Experimental design: competition cultures were started with WT and mutant strains mixed at an approximately 1:1 ratio with each strain expressing a different fluorescent protein. The proportion of each strain in the mixed culture was measured over time by flow cytometry (B), and plotted as the percent of mutant cells quantified after growth in (C) 45′:45′ LD and (D) continuous light conditions. Error bars represent mean ± SEM.

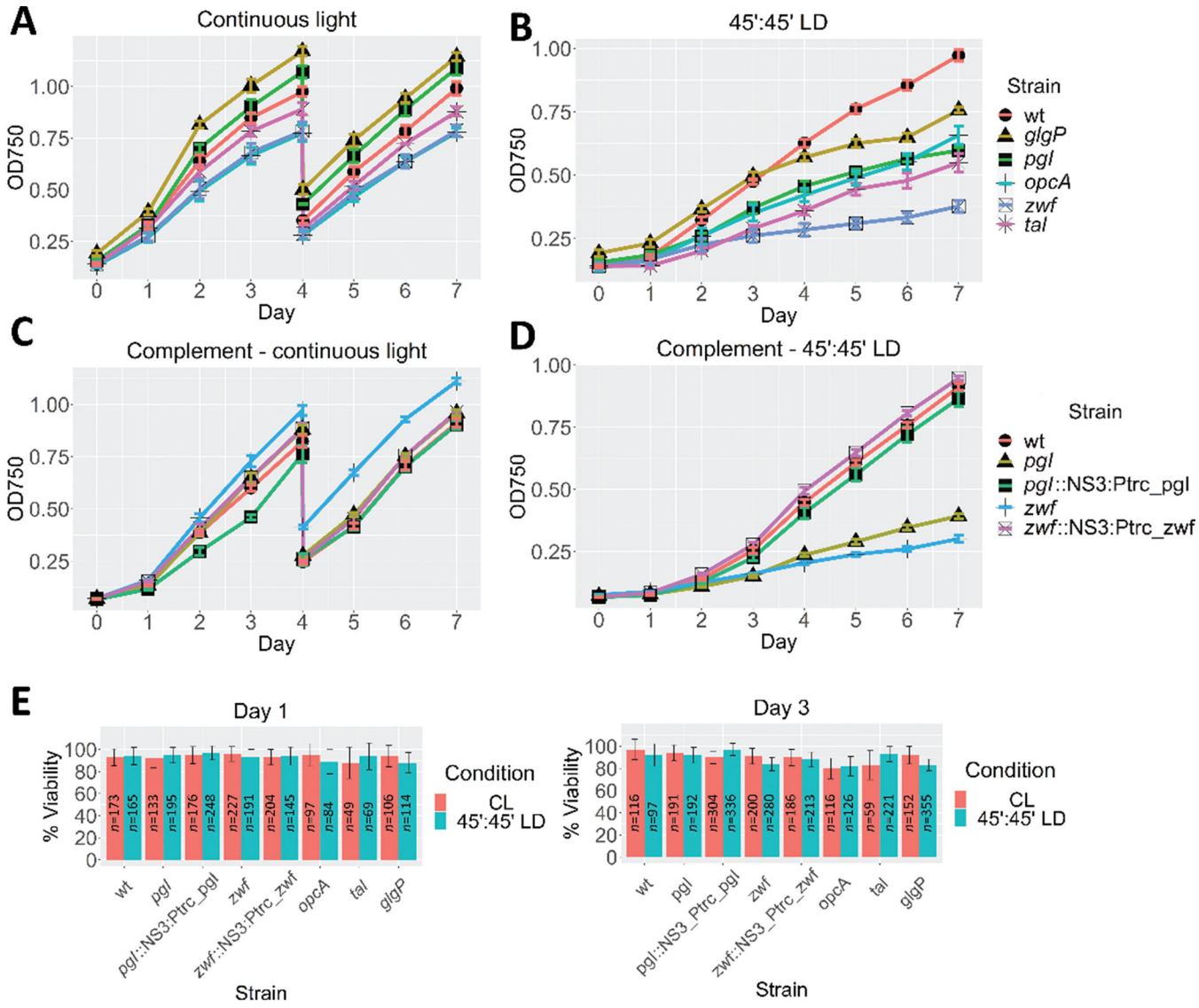


**Fig. 5.**

Growth rates of OPPP and glycogen metabolism mutants and complemented mutant strains. OPPP and glycogen metabolism mutant strains were grown alongside WT *S. elongatus* in (A) continuous light or (B) 45′:45′ LD. Cultures in continuous light were diluted 1:4 with fresh medium on day 4 to prevent self-shading at high culture density. The *pgl* and *zwf* mutant strains and the complemented strains were grown in (C) continuous light and (D) 45′:45′ LD. Error bars represent mean ± SEM. (E) Cell viability was measured by fluorescence microscopy of autofluorescence on days 1 and 3 after exposure to continuous light or 45′:45′ LD. Error bars represent standard deviation of the total cell count.

## Table 1

RB-TnSeq 45’ :45’ LD gene fitness.

| | | $T_0$ analysis | | |
|---|---|---|---|---|
| **Gene** | **Annotation** | **Rank (negative fitness)** | **Fitness** | **log.fdr** |
| Synpcc7942_0401 | *dgkA* | 1 | −3.397295428 | 1.26E-160 |
| Synpcc7942_1628 | conserved hypothetical | 2 | −3.040051151 | 1.34E-61 |
| Synpcc7942_0529* | *PgI* | 3 | −2.750369456 | 1.5E-63 |
| Synpcc7942_2334* | *zwf* | 4 | −2.560880331 | 1.46E-254 |
| Synpcc7942_0244* | *glgP* | 5 | −2.471957561 | 0 |
| Synpcc7942_2333* | *opcA* | 6 | −2.262700532 | 3.42E-136 |
| Synpcc7942_2297* | *tal* | 7 | −2.24107901 | 1.22E-71 |
| Synpcc7942_1218 | *kaiA* | 482 | −0.42728 | 1.5E-10 |
| Synpcc7942_2380 | conserved hypothetical | 1634 | −0.1707 | 1.62E-08 |

Genes marked with an askerisk are those shown in red in Fig. 3C and E.